การเปรียบเทียบผลการวิเคราะห์ระหว่างระเบียบวิธีไฟไนต์เอลิเมนต์และวิธีโฟโตอิลาสติกซิตี้ สำหรับปัญหากลศาสตร์การสัมผัสใน 2 มิติ

วิโรจน์ ลิ่มตระการ [1] บรรจง เดชาพานิชกุล [2]

มหาวิทยาลัยธรรมศาสตร์ ศูนย์รังสิต ต.คลองหนึ่ง อ.คลองหลวง จ.ปทุมธานี 12120

สุธี โอฬารฤทธินันท์ [3] สุวัฒน์ จีรเธียรนาถ [4] และ วุฒิพงษ์ รังษีสันติวานนท์ [4]

ศูนย์เทคโนโลยีโลหะและวัสดุแห่งชาติ

อุทยานวิทยาศาสตร์ ถ.พหลโยธิน ต.คลองหนึ่ง อ.คลองหลวง จ.ปทุมธานี 12120

บทคัดย่อ

บทความนี้กล่าวถึงการประยุกต์ระเบียบวิธีไฟไนต์เอลิเมนต์และวิธีโฟโตอีลาสติกซิตี้เพื่อหาค่าการเคลื่อนตัวและการกระจายความเค้นที่เกิดขึ้นในปัญหากลศาสตร์การสัมผัส โดยเริ่มจากทฤษฎีต่างๆ ที่เกี่ยวข้อง ได้แก่ ทฤษฎีกลศาสตร์การสัมผัสใน 2 มิติ การหาสมการไฟไนต์เอลิเมนต์ที่ได้จากวิธีตัวคูณลากรางจ์และพีนอลที ขั้นตอนการคำนวณและการประยุกต์เงื่อนไขขอบเขต จากนั้นอธิบายถึงทฤษฎีโฟโตอีลาสติกซิตี้ ต่อมาแสดงผลการประยุกต์กับปัญหา 2 ตัวอย่าง คือ ปัญหาแผ่นวงกลมสัมผัสกัน และปัญหาการสัมผัสกันระหว่างแผ่นวงกลมและแผ่นเรียบ ผลการคำนวณจากระเบียบวิธีไฟไนต์เอลิเมนต์ได้เปรียบเทียบกับผลการคำนวนจากทฤษฎีของเฮิร์ตซ และวิธีโฟโตอิลาสติกซิตี้ ผลลัพธ์ที่ได้จากการประยุกต์ทั้ง 2 เทคนิคแสดงให้เห็นถึงผลลัพธ์ที่สอดคล้องกัน

คำสำคัญ : ระเบียบวิธีไฟไนต์เอลิเมนต์ / โฟโตอีลาสติกซิตี้ / กลศาสตร์การสัมผัส

---

[1] *ผู้ช่วยศาสตราจารย์ ภาควิชาวิศวกรรมเครื่องกล E-mail: limwiroj@engr.tu.ac.th*

[2] *นักศึกษาปริญญาโท ภาควิชาวิศวกรรมเครื่องกล*

[3] *วิศวกร*

[4] *นักวิจัย*

Comparison of Finite Element Solution and Photoelastic Results for 2-D Contact Mechanics Problems

Wiroj Limtrakarn [1], Bunjong Dechapanichkul [2],
Thammasat University, Rangsit Campus, Klong 1, Klong Luang, Pathum Thani 12121
Sutee Olarnrithinun [3], Suwat Jirathearanat [4], and Wuttipong Jirathearanat [4]
National Metal and Materials Technology Center, Thailand Science Park,
Paholyotin Road, Klong 1, Klong Luang, Pathum Thani 12120

Abstract

The finite element method and photoelasticity technique are presented to predict displacement and stress distribution for contact mechanics problems. The paper first describes 2D contact mechanics theory. The finite element formulations based on Lagrange multiplier and Penalty method are presented, The computational procedure and its boundary conditions are then described. The photoelasticity theory and its procedure are also explained. To evaluate the efficiency of both techniques, the displacement and stress distribution for two circular plates contact problem and circular-flat plate contact problem are used to compare the finite element solutions and those from photoelasticity technique and Hertz solution. The solutions show that the stress distributions predicted by finite element method are in good agreement with the photoelasticity results and Hertz solutions.

Keywords : Finite Element Method / Photoelasticity / Contact Mechanics

[1] *Assistant Professor, Department of Mechanical Engineering. E-mail: limwiroj@engr.tu.ac.th*
[2] *Master Degree Student, Department of Mechanical Engineering.*
[3] *Engineer.*
[4] *Researcher.*

1. Introduction

In solid mechanics problems, the contact condition between two surfaces is one of important factors that affects the maximum stress in static loading or wear in dynamic loading. A correct understanding in the contact behavior under static loading can be directly implemented on the product design and can be extended to use with the contact behavior under dynamic loading such as sheet metal stamping process. The finite element method has been employed to predict the contact behavior for several years. Consequently, there are many finite element algorithms invented to predict the contact behavior in static loading such as Penalty algorithm, Lagrange multiplier algorithm and augmented Lagrange multiplier, and etc.

This paper studied the capability and performance of contact algorithms for solving 2D contact problems. The finite element method for 2D contact mechanics is presented. The computational procedure and its boundary conditions are shown. Two contact algorithms (Penalty algorithm and Lagrange multiplier algorithm) are used in displacement and stress distribution analysis for two deformable circular plate contact problem and a deformable circle plate in contact with a deformable rectangular plate problem. Then, the computational results are validated with Hertz solution and photoelasticity.

2. Theory

2.1 Governing differential equation

Contact mechanics is governed by the equilibrium equations, strain-displacement relations and constitutive equations.

2.1.1 Equilibrium equations

The equilibrium equations can be written in variational form as [1],

$$\delta W_S - \delta W_R - \delta W_C = \int_\Omega \sigma_{ij} \delta e_{ij} d\Omega - \int_S t_i \delta u_i dS = 0 \quad (1)$$

where δW_S, δW_R and δW_C are virtual energy of internal stress, external force and contact, respectively. σ_{ij}, is the stress components, δe_{ij} is virtual strain, t_j is the surface traction, and δu_i is virtual displacement. Boundary conditions may consist of specifying the surface traction [2] as depicted in Fig. 1 as,

$$\sigma_{ij} n_i = t_1 \quad (2)$$

where n_i and t_1 are the outward unit normal vector and surface traction on the boundary S_1 at time t, respectively. The boundary condition may include the prescribed displacement on the boundary S_2 as,

$$u_i(x,t) = u_2(t) \quad (3)$$

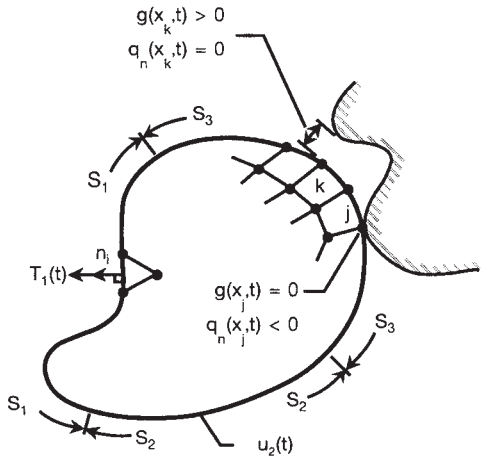

Fig. 1 Boundary conditions for contact mechanics problem.

Also along the contact boundary S_3, the normal contact stress should be compressive and the boundary should not penetrate into the other as follows,

$$q_n(x,t) = q_c(x,t)\, n_i \leq 0 \quad (4)$$

$$g(x,t) = g(x) - u(x,t)\, n_i \geq 0 \quad (5)$$

where $q_c(x,t)$ is the contact traction, $q_n(x,t)$ is the normal component of contact traction, and $g(x,t)$ is the gap between the two boundary surfaces.

The equation 4 and 5 are the contact condition of Lagrange multiplier method. This method expresses the virtual work in the form,

$$\delta W_C = \int_S \delta(\lambda_N g_N + \lambda_T g_T) dS \quad (6)$$

where λ is the Lagrange multiplier and equivalent to the reaction force at contact point.

The other contact algorithm is Penalty method. It will allow very small penetration occurs on contact surface.

$$g(x,t) = g(x) - u(x,t)\, n_i = 0 \quad (7)$$

$$\delta W_C = \int_S (\varepsilon_N g_N \delta g_N + t_T \delta g_T) dS \quad (8)$$

where ε is the Penalty parameter, subscript N and T mean normal and tangential direction, respectively. Equation 8 is valid under slip condition. If the contact condition is pure stick then $t_T = \varepsilon_T g_T$.

2.1.2 Strain-displacement relations

Contact problem normally involve small strain and assume the strain-displacement relations in the form,

$$\varepsilon_{ij} = \frac{1}{2}(u_{i,j} + u_{j,i}) \quad (9)$$

where ε_{ij}, is the strain components; u_i, and u_j, are the displacement components.

2.1.3 Constitutive equations

Contact mechanics has the constitutive equation that shows the relation of elastic strain, ε_{ij} and the elastic stress, σ_{ij} in the form,

$$\{\sigma\} = [C]\{\varepsilon\} \quad (10)$$

where [C] is the elasticity matrix [3].

2.2 Finite Element Equations

The weak form of virtual work principle [2] is applied to the equilibrium equation 1 and written in matrix form as,

$$[K]\{U\} = \{U\} + \{F_c\} \quad (11)$$

where [K] is the stiffness matrix, {U} is the displacement vector, {F}is the external load vector, and $\{F_c\}$ is the load vector of contact force.

2.3 Photoelasticity [4, 5]

Photoelasticity technique can be explained with the wave theory of light in the form of harmonic waveform.

$$E = A\cos(\phi - \omega t) \tag{12}$$

where E is magnitude of light wave, A is the wave amplitude, ϕ is the phase angle of wave, ω is angular frequency, and t is time.

$$\phi = \frac{2\pi}{\lambda}(z + \delta) \tag{13}$$

$$\omega = 2\pi f = \frac{2\pi v}{\lambda} \tag{14}$$

where z is position along propagation axis, λ is wavelength, δ is phase of wave, f is wave frequency and v is wave velocity.

Photoelasticity technique will control light path from source through wave plates and measured model is located in the middle of them as shown in Fig. 2.

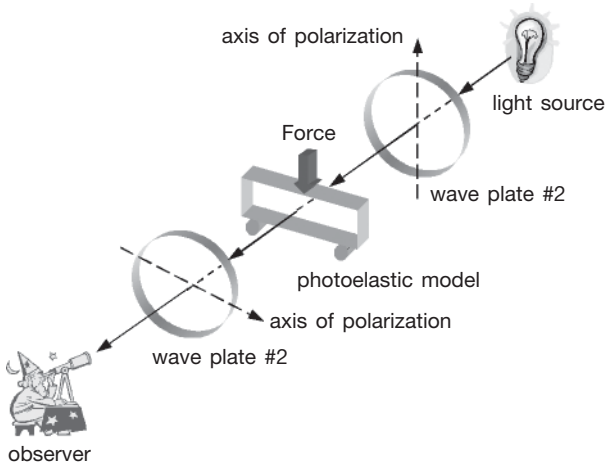

Fig. 2 A photoelastic model in a plane optical components.

A wave plate resolves an incident light wave into parallel and perpendicular components to the axis of polarization. The parallel component is transmitted, while the other component is internally absorbed.

After the light wave entering the photoelastic model under loading, the stressed model exhibits similar optical properties of a wave plate. The incident light wave is resolved into parallel and perpendicular components to the principal stress directions at the point. After leaving the photoelastic model, the two light wave components with different velocities enter the wave plate #2 and are resolved again.

The leaving light wave has a relative retardation or angular phase shift, Δ in the following equation.

$$\Delta = \frac{2\pi}{\lambda}\delta = \frac{2\pi h}{\lambda}(n_2 - n_1) \quad \textbf{(15)}$$

where h is the wave plate thickness, and n is the refractive index of media.

The principal stresses is related to the refractive index in the form,

$$n_2 - n_1 = c(\sigma_1 - \sigma_2) \quad \textbf{(16)}$$

Equation 16 is called stress-optic law. c is the relative stress-optic coefficient, σ_1 and σ_2 are the major and minor principal stress, respectively.

After substituting equation 16 into equation 15, the equation is in the form,

$$\sigma_1 - \sigma_2 = \frac{Nf_\sigma}{h} \quad \textbf{(17)}$$

where N is the number of fringes appearing in an isochromatic fringe pattern and f_σ is the material fringe value.

$$N = \frac{\Delta}{2\pi} = \frac{\delta}{\lambda} \quad \textbf{(18a)}$$

$$f_\sigma = \frac{\lambda}{c} \quad \textbf{(18b)}$$

3. Examples

This paper focuses on two contact algorithms for finite element analysis, Penalty method and Lagrange multiplier method. The efficiency of each method is studied and compared with Hertz solutions in the first example. The examples used in this paper are two circular plates contact problem and circular-flat plate contact problem.

3.1 Two circular plates contact problem

As shown in Fig. 3, two deformable circular plates are in contact. A force of 110.8 N is applied on the top circle while the bottom circle lies on the rigid floor. Both circles have the same material properties and dimensions, ie. Young's Modulus = 952.889 MPa, Poisson's ratio = 0.38 and radius = 25 mm.

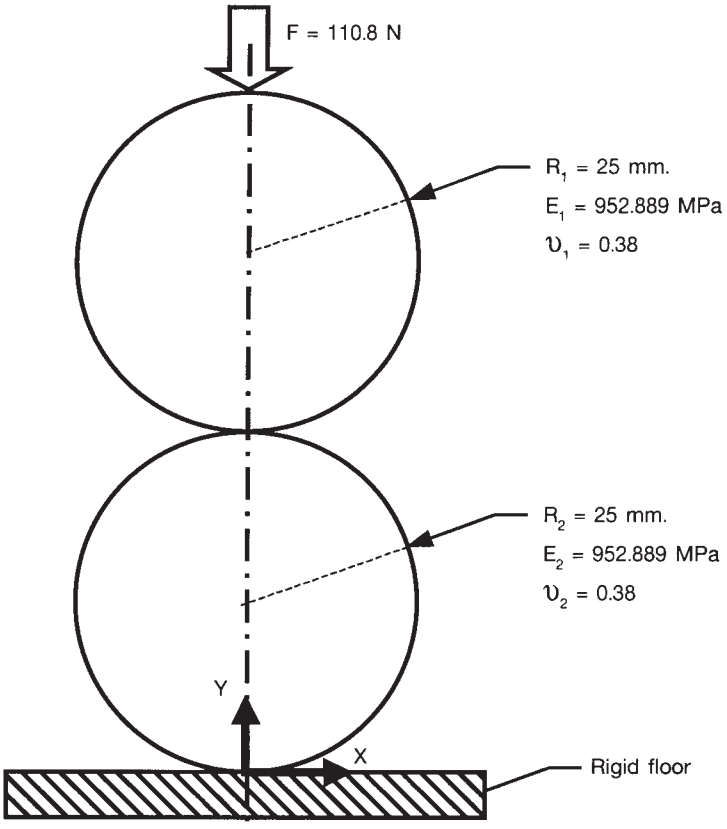

Fig. 3 Two circle plate contact problem statement.

The contact behavior between two circles is investigated and has the solution based on Hertz theory in the form,

$$a = 2\sqrt{\frac{F}{l}\cdot\frac{1}{\pi}\cdot\frac{(1-\upsilon_1^2)/E_1 + (1-\upsilon_2^2)/E_2}{1/R_1 + 1/R_2}} \quad \textbf{(19a)}$$

$$b = 0.638\frac{F}{l}\cdot\left(\frac{1-\upsilon_1^2}{E_1}\right)\cdot\left[\frac{2}{3} + \ln\frac{2R_1}{a} + \ln\frac{2R_2}{a}\right] \quad \textbf{(19b)}$$

where a is the contact length and b is the displacement of top circular plate in y direction.

The finite element model consists of 5,360 nodes and 5,280 elements for a half right model. Fig. 7 shows details of elements near the contact surface.

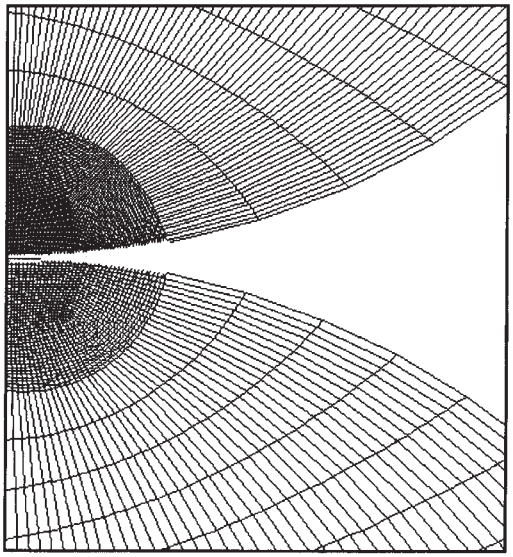

Fig. 4 Finite element model around contact surface.

Applied forces are set at 27.7 N, 55.4 N, 83.1 N, and 110.8 N following the force scale of the photoelasticity equipment. The deformation solution is compared with Hertz theory. Fig. 5 shows the relation of contact length and applied forces. The solution error from the Penalty method is 0.7%, which is much less than that of Lagrange multiplier method (10%). Fig. 6 displays displacement along y axis versus the applied force. When comparing the solutions with Hertz theory, Penalty and Lagrange multiplier methods show a comparable level of accuracy.

Although, more accurate solution can be obtained by reducing the element size around the contact surface, however, the smaller element size, the more expenses in CPU time and space storage are required.

For stress analysis, the solutions from both Penalty and Lagrange multiplier methods are identical. Fig. 7 shows the normal stress along the y axis. Fig. 8 displays the normal stress y along the circumference.

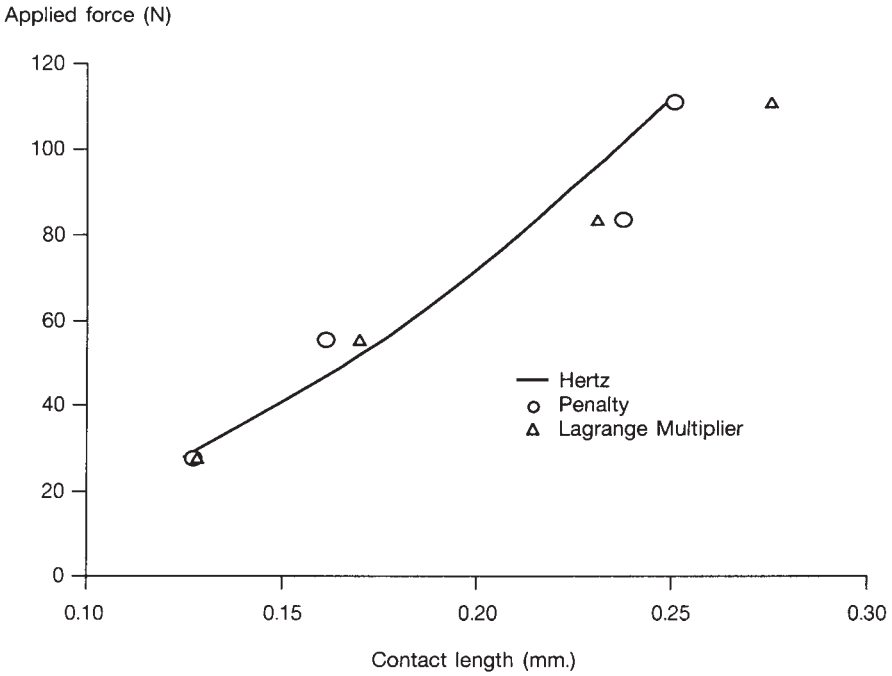

Fig. 5 Plot of applied force and contact length.

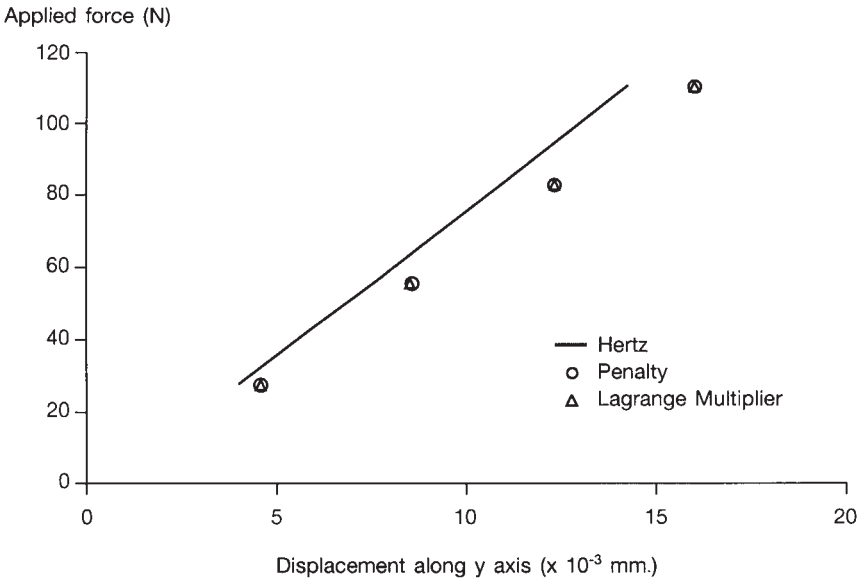

Fig. 6 Plot of applied force and displacement in y axis.

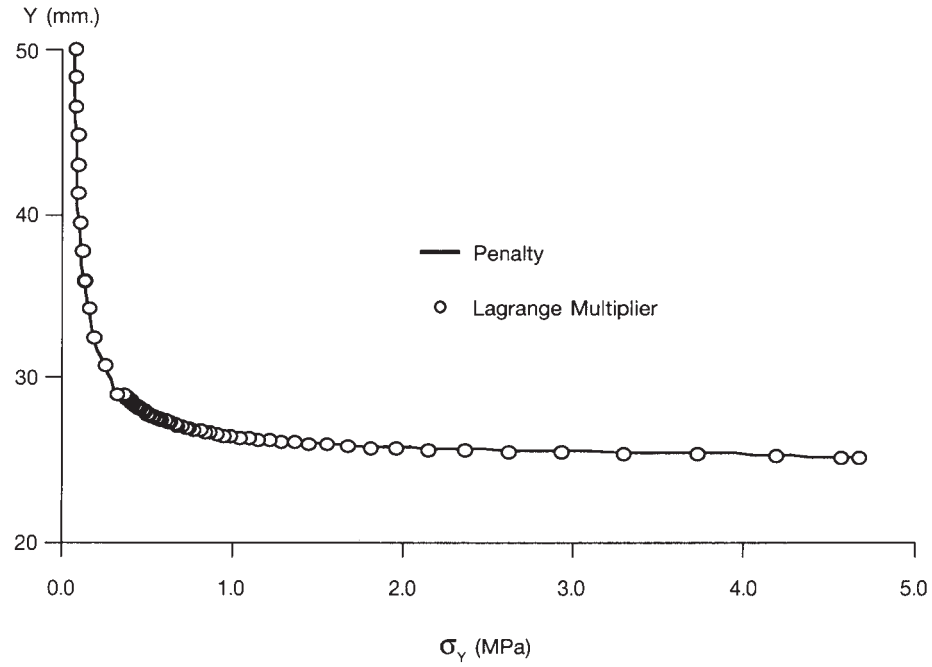

Fig. 7 Plot of normal stress (σ_Y) along y axis.

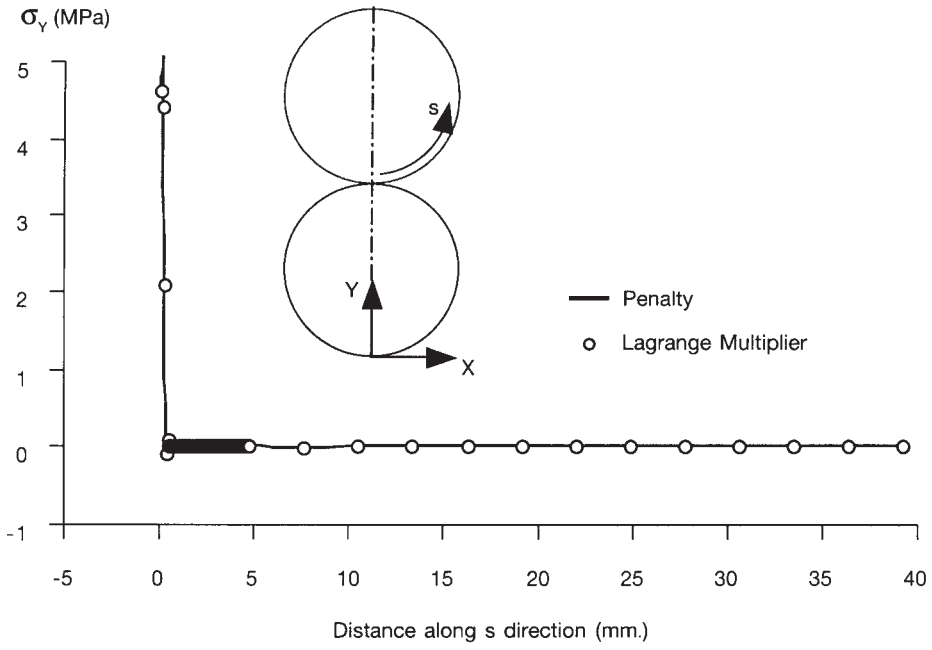

Fig. 8 Plot of normal stress (σ_Y) along s direction.

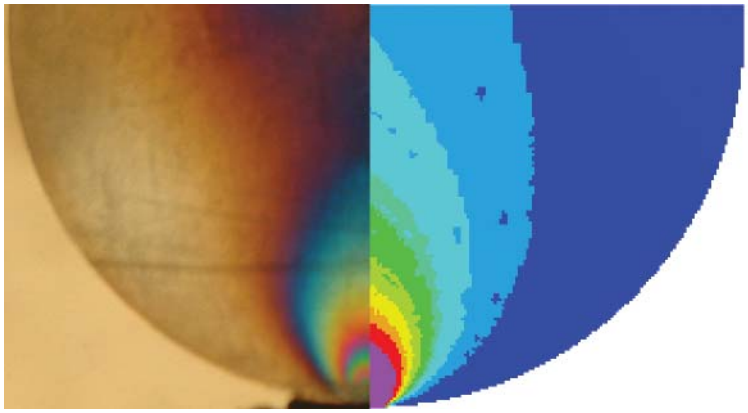

Photoelasticity Finite Element Method

Fig. 9 Comparison of max shear stress between photoelasticity result and finite element method solution.

Fig. 9 shows the maximum shear stress contours of the photoelasticity result and finite element solution based on 110.8 N applied on the top circle. As the result suggested, both results have a good agreement.

3.2 Circular-flat plate contact problem

A circular plate is applied with a force in y direction against a deformable flat plate which is supported by two rigid rollers as shown in Fig. 10. Because of symmetry, the finite element model is generated only the right half of the model and consists of 5,580 nodes and 5,450 elements.

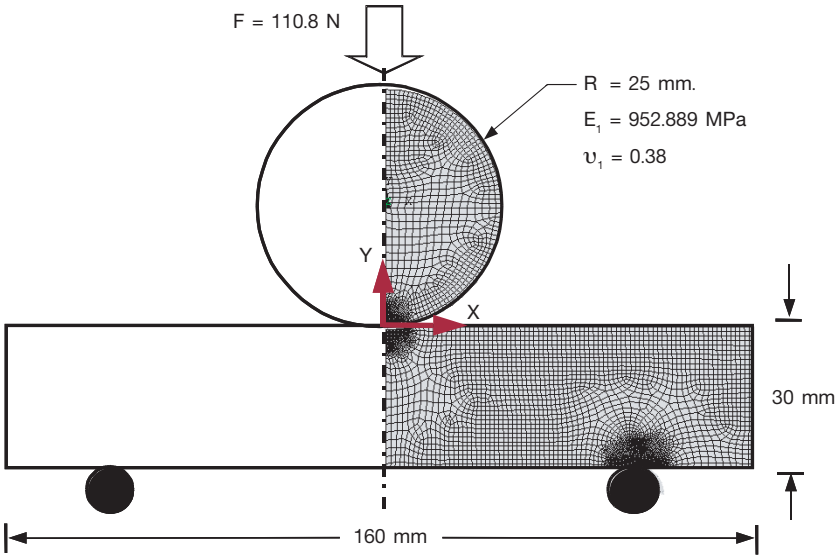

Fig. 10 Circular-flat plate contact problem.

Near the contact surface area will occur stress and displacement behavior based on contact theory, while the behavior at the bottom edge of the flat plate is based on bending theory. The finite element solution agrees well with the result from photoelasticity technique as shown by maximum shear stress contours in Fig. 11. According to the results of the Penalty and Lagrange multiplier method, the accuracy of both methods is equally the same as shown in Fig. 12-15. Contact lengths and displacement along y axis will increase as the applied forces is larger as shown in Fig. 12 and 13. The maximum normal stress in the y direction will occur at the contact point (y = 0 mm.) and decreases along the y axis away from the contact point, as shown in Fig. 14 and 15.

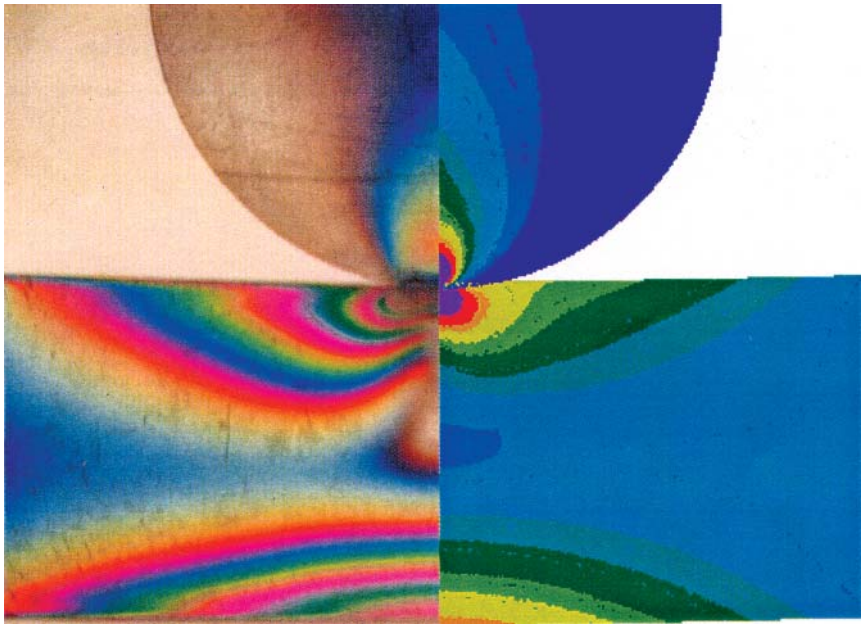

Photoelasticity Finite Element Method

Fig. 11 Comparison of max shear stress between photoelasticity result and finite element method solution.

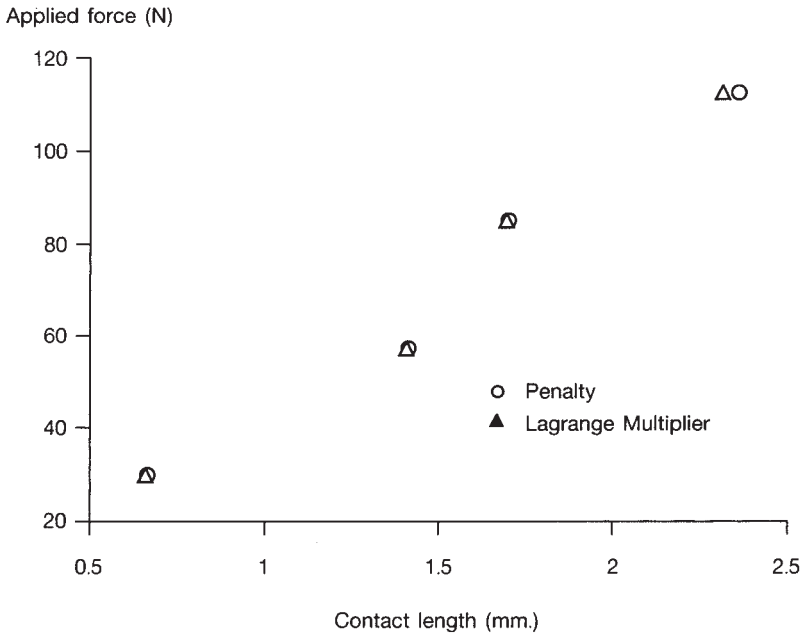

Fig. 12 Plot of applied force and contact length

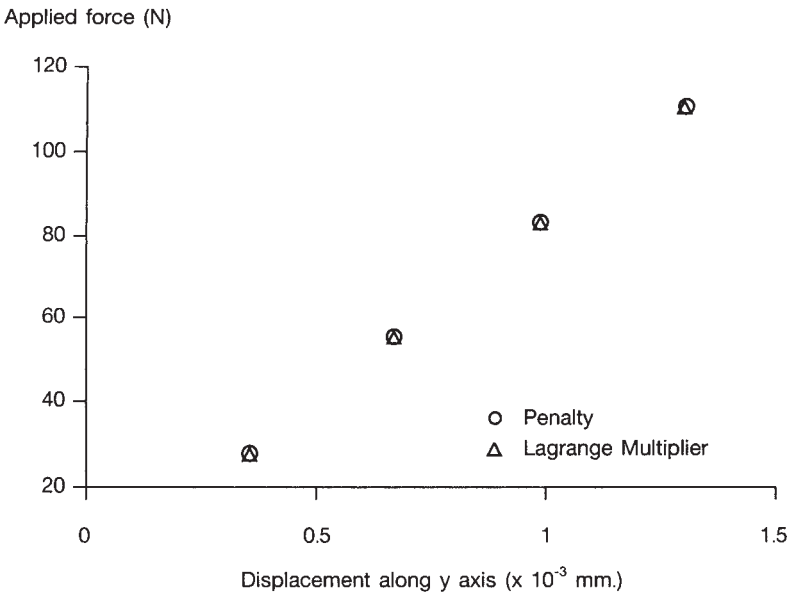

Fig. 13 Plot of applied force and displacement in y axis.

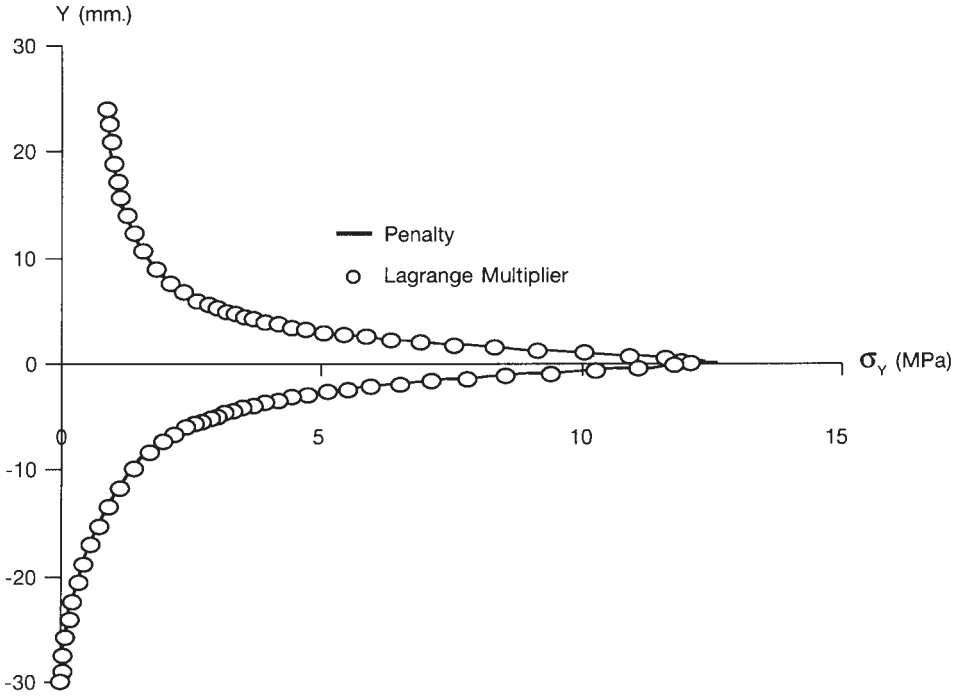

Fig. 14 Plot of normal stress (σ_Y) along y axis.

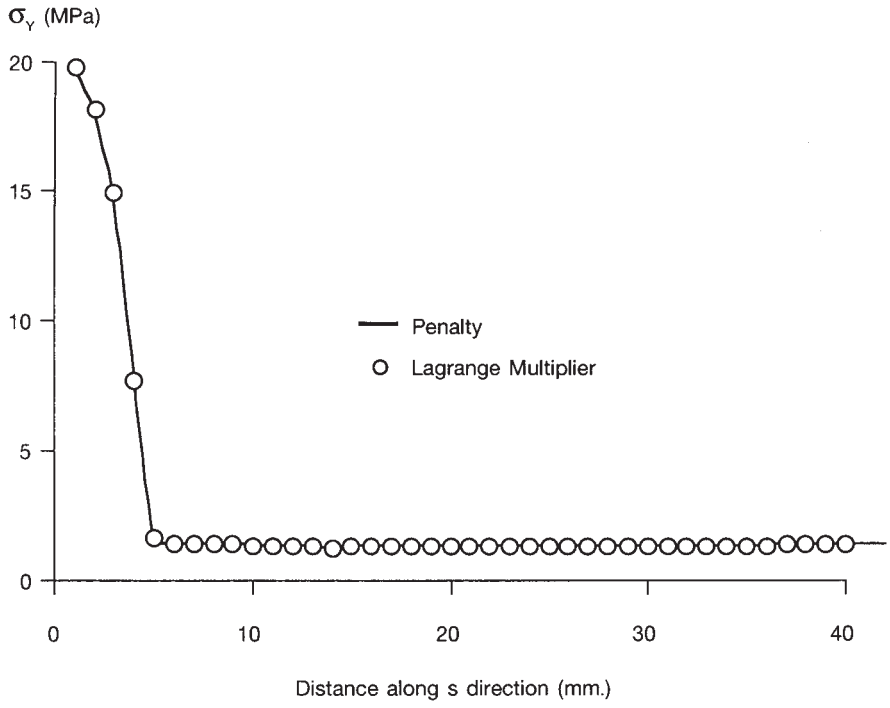

Fig. 15 Plot of normal stress (σ_Y) along s direction.

4. Conclusions

This paper presents the finite element method and photoelasticity method in solving contact mechanics problems. Examples are two circular plate contact problem and circular-flat plate contact problem. Results show that the Penalty and Lagrange multiplier methods can be used to predict the contact behavior efficiently. Computational results are compared with the Hertz theory and photoelasticity result and show a good agreements.

5. Acknowledgements

The authors are pleased to acknowledge Thailand Graduate Institute of Science and Technology (TGIST) and National Metal and Materials Technology Center (MTEC) for supporting this research work.

6. References

1. Fung, Y. C., 1965, *Foundations of Solid Mechanics*, International Edition, Prentice-Hall.

2. Zhong, Z. H., 1993, *Finite Element Procedures for Contact-Impact Problems*, Oxford University Press, Oxford, UK.

3. Zienkiewicz, O. C. and Taylor, R. L., 2004 *The Finite Element Method*, Fourth Ed., Vol. I, McGraw-Hill Press, Singapore.

4. Dally, J. W. and Riley, W. F., 1991, *Experimental Stress Analysis*, Third Edition, McGraw-Hill Press, Singapore.

5. Limtrakarn, W., 2005, "Comparison in the Stress Analysis of 2D Solid Mechanics Problems of Finite Element Method and Photoelasticity", *KMUTT Research and Development Journal*, Vol. 28, No. 1, pp. 75-86.

6. Dechaumphai, P., 2004, *Finite Element Method in Engineering*, Third Ed., Chulalongkorn University Press, Bangkok, Thailand.

7. Wriggers, P., 2002, *Computational Contact Mechanics*, John Wily & Sons.